

Searching for decaying dark matter in deep *XMM-Newton* observation of the Draco dwarf spheroidal

Oleg Ruchayskiy¹, Alexey Boyarsky², Dmytro Iakubovskiy³,
Esra Bulbul⁴, Dominique Eckert⁵, Jeroen Franse^{2,6},
Denys Malyshev⁵, Maxim Markevitch⁷, Andrii Neronov⁵

¹Ecole Polytechnique Fédérale de Lausanne

FSB/ITP/LPPC, BSP 720, CH-1015, Lausanne, Switzerland

²Instituut-Lorentz for Theoretical Physics, Universiteit Leiden

Niels Bohrweg 2, Leiden, The Netherlands

³Bogolyubov Institute of Theoretical Physics, Metrologichna Str. 14-b, 03680, Kyiv, Ukraine

⁴Kavli Institute for Astrophysics and Space Research,

Massachusetts Institute of Technology, 77 Massachusetts Avenue, Cambridge, MA 02139

⁵Department of Astronomy, University of Geneva, ch. d'Ecogia 16, CH-1290 Versoix, Switzerland

⁶Leiden Observatory, Leiden University, Niels Bohrweg 2, Leiden, The Netherlands

⁷NASA Goddard Space Flight Center, Code 662, 8800 Greenbelt Rd., Greenbelt, MD 20771, USA

Abstract

We present results of a search for the 3.5 keV emission line in our recent very long (~ 1.4 Ms) *XMM-Newton* observation of the Draco dwarf spheroidal galaxy. The astrophysical X-ray emission from such dark matter-dominated galaxies is faint, thus they provide a test for the dark matter origin of the 3.5 keV line previously detected in other massive, but X-ray bright objects, such as galaxies and galaxy clusters. We do not detect a statistically significant emission line from Draco; this constrains the lifetime of a decaying dark matter particle to $\tau > (7 - 9) \times 10^{27}$ s at 95% CL (combining all three *XMM-Newton* cameras; the interval corresponds to the uncertainty of the dark matter column density in the direction of Draco). The PN camera, which has the highest sensitivity of the three, does show a positive spectral residual (above the carefully modeled continuum) at $E = 3.54 \pm 0.06$ keV with a 2.3σ significance. The two MOS cameras show less-significant or no positive deviations, consistently within 1σ with PN. Our Draco limit on τ is consistent with previous detections in the stacked galaxy clusters, M31 and the Galactic Center within their $1 - 2\sigma$ uncertainties, but is inconsistent with the high signal from the core of the Perseus cluster (which has itself been inconsistent with the rest of the detections). We conclude that this Draco observation does not exclude the dark matter interpretation of the 3.5 keV line in those objects.

1 Introduction

A spectral feature at energy $E \sim 3.5$ keV has recently been observed in the long-exposure X-ray observations of a number of dark matter-dominated objects: in a stack of 73 galaxy clusters [1] and in the Andromeda galaxy and the Perseus galaxy cluster [2]. The possibility that this spectral feature may be the signal from decaying dark matter has sparked a lot of interest in the community, and many dark matter models explaining this signal have been proposed (see e.g. [3] and refs. therein). The signal was subsequently detected in the Galactic Center [4–7], in the center of the Perseus galaxy cluster with *Suzaku* [8], in a stacked spectrum of a new set of galaxy clusters [9], but not found in stacked spectra of dwarf spheroidal galaxies [10], in outskirts of galaxies [11], in the XRB [12, 13].

There are three classes of non-dark matter explanations: a statistical fluctuation, an unknown systematic effect or an atomic line. Instrumental origins of this signal have been shown to be unlikely for a variety of reasons: the signal is present in the spectra of galaxy clusters in all of *XMM-Newton* detectors and also in *Chandra*, yet it is absent in a very-long exposure *XMM-Newton* [2] or *Suzaku* [13] blank sky backgrounds. The position of the line in galaxy clusters scales correctly with redshift [1, 2, 9], and the line has radial surface brightness profiles in the Perseus cluster (except its core [1]) and Andromeda galaxy [2] consistent with our expectations for decaying dark matter and with the mass distribution in these objects.

The astrophysical explanation of this signal (e.g., an anomalously bright K XVIII line [1, 4–7, 9] or Ar XVII satellite line [1], or a Sulfur charge exchange line [14]) require a significant stretch of the astrophysical emission models, though they can be unambiguously tested only with the high spectral resolution of the forthcoming *Astro-H* and *Micro-X* [12, 15–18] microcalorimeters.

The dark matter interpretation of the origin of the line allows for non-trivial consistency check by comparing observations of different objects: the intensity of the line should correlate with the *dark matter column density* – a quantity that is bracketed between roughly $10^2 M_\odot/\text{pc}^2$ and $\text{few} \times 10^3 M_\odot/\text{pc}^2$ for all objects from smallest galaxies for larger clusters [19, 20]. For example, the observation of the 3.5 keV line in M31 and the Perseus cluster puts a *lower limit on the flux* expected from the Galactic Center (GC). On the other hand, the non-detection of any signal in the off-center observations of the Milky Way halo (the blank sky dataset of [2]) *provides an upper limit* on the possible flux from the GC, given the observational constraints on the DM distribution in the Galaxy. Ref. [5] demonstrated the flux of the 3.5 keV line detected in the GC, falls into this range.

To study this question further, we observed the central $r = 14'$ of the Draco dwarf spheroidal galaxy with *XMM-Newton* with a very deep exposure of 1.4 Msec. Dwarf spheroidal galaxies (dSphs) are the most extreme dark matter-dominated objects known. The observations of thousands of stars in the “classical” dwarf satellites of the Milky Way make possible the determination of their DM content with very low uncertainties, with the Draco dSph being one of the best studied (see [21] for the latest mass modeling). The relatively small uncertainty on the dark matter column density in Draco and its “darkness” in X-rays due to lack of gas or X-ray binaries allows us to devise a test of the decaying dark matter interpretation of the ~ 3.5 keV line, as we have a clear prediction of the expected line flux for Draco based on the masses of this galaxy and the other objects.

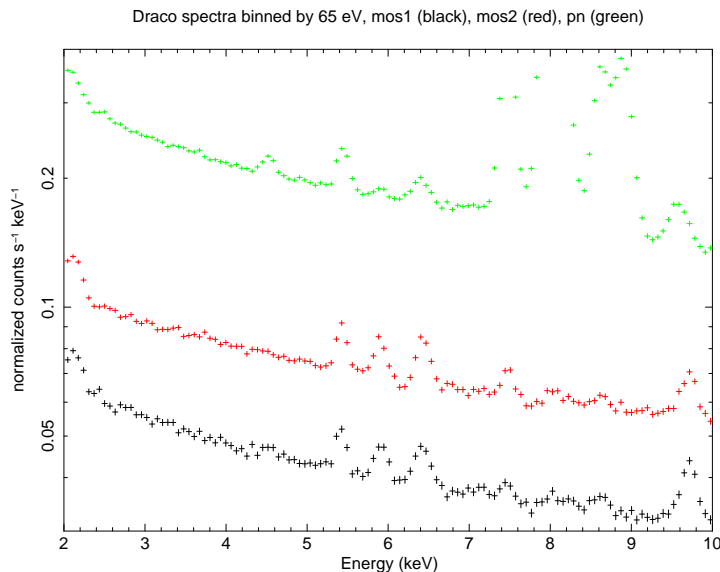


Figure 1: Spectra of Draco dwarf spheroidal seen by MOS1 (black), MOS2 (red) and PN (green) cameras.

A clear detection of the ~ 3.5 keV line in Draco would provide very convincing evidence for the decaying DM interpretation, as there is no known physical process that would produce *the same signal* over such a broad range of objects and environments, with an intensity that scales with the DM content, from galaxy clusters of huge masses and large abundances of hot gas, through spiral galaxies, and then all the way down to dwarf galaxies of very low magnitude and negligible gas content.

The estimated column density within the central $14'$ is a factor of a few lower in dSphs (including Draco) than in the centers of nearby spiral galaxies or clusters (albeit has a much lower uncertainty). Therefore, to achieve the same signal-to-noise for a dSph as for a spiral galaxy for all observationally possible ratios of the DM column density, one would need a prohibitively long observation. The uncertainty in DM content of the galaxies becomes crucial. Therefore, the raw exposure time of the Draco observation (1.4 Msec) has been chosen in such a way as to provide only marginal detection in the case of the weakest possible line (compatible with previous observations).

In this paper we describe the results of the analysis of these Draco observations. We do find weak positive residuals at the predicted energy above the (carefully-modeled) continuum in the PN spectrum and in one of the two MOS spectra, but at a low statistical significance that allows only an upper limit on the line flux to be set. The upper limit is consistent with most of the previous positive line detections, thus, we *cannot exclude dark matter decay* as origin of the 3.5 keV line.

2 Results

The data preparation and analysis is fairly standard and is described in Appendix A. The extracted spectra are shown in Fig. 1. They are dominated by the instrumental and Cosmic (CXB) X-ray backgrounds, which we will carefully model below to see if there

Camera	Raw exp. [Msec]	Cleaned exp. [Msec]	FoV [arcmin ²]
MOS1	1.43	0.97	318.9
MOS2	1.44	1.02	573.5
PN	1.29	0.65	543.9

Table 1: Dataset, 26 observations of *XMM-Newton* AO14. Although PN camera has the lowest exposure, it has the highest number of counts/bin in the region of interest (c.f. Fig. 1).

is any residual flux at 3.5 keV. As has been stressed in our previous works, the 3.5 keV line feature is so weak that the continuum in its spectral vicinity has to be modeled to a very high precision to be able to detect the line – more precisely than what’s acceptable in the usual X-ray observation.

The basic information about the spectra is listed in Table 1. As a baseline model, we used the combination of Cosmic X-ray Background (extragalactic `powerlaw` folded with the effective area of the instrument) and instrumental background (instrumental `powerlaw` not folded with instrument response, plus several narrow `gaussians` describing fluorescence lines) components. The model parameters are summarized in Table 5; they are consistent with previous measurements and consistently vary among MOS1, MOS2 and PN cameras. Particular differences of the models among individual cameras are described below.

2.1 Line detection in PN camera

We obtained an excellent fit to the EPIC PN spectrum, with $\chi^2 = 47.0$ for 58 d.o.f. (Table 5). The spectrum shows a faint line-like residual at the right energy, $E = 3.54_{-0.05}^{+0.06}$ keV. Its flux is

$$F_{\text{PN}} = 1.65_{-0.70}^{+0.67} \times 10^{-6} \text{ cts/sec/cm}^2 \quad \text{or} \quad 3.0_{-1.29}^{+1.23} \times 10^{-9} \text{ cts/sec/cm}^2/\text{arcmin}^2 \quad (1)$$

(where the second value corresponds to the surface brightness). The improvement of fit when adding the line is $\Delta\chi^2 = 5.3$. Thus, the detection is only at a 2.3σ significance. The PN spectrum with the unmodeled line-like residual together with the $\Delta\chi^2 = 1, 4, 9$ contours is shown in Figure 2. In this Figure, we show only 2.8-6.5 keV range for clarity, while the fit includes higher energies, as described in Appendix A.

2.2 MOS cameras

Next we turn to MOS1 and MOS2 cameras. In MOS2 camera, we detected line-like residuals at ~ 3.38 keV (significance 3.2σ) and ~ 3.77 keV (significance 3.5σ), see Table 5 in Appendix A. The positions of these residuals are consistent with K $K\alpha$ and Ca $K\alpha$ fluorescent lines, respectively. These fluorescent lines have not been previously detected in the MOS cameras, but have been detected in the PN camera with the enhanced calibration source (the so-called `Ca1Closed` mode, see Fig. 6 of [22] for details). Another line-like residual at ~ 3.05 keV is visible (in the MOS2 spectrum only) at a 1.9σ significance; we could not identify it, though its energy is consistent with L and M lines of several heavy

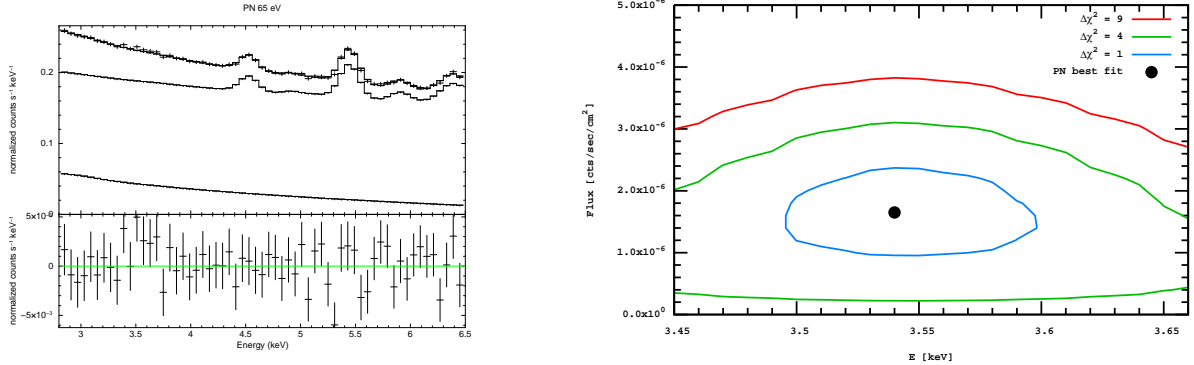


Figure 2: Left panel: PN spectrum with *unmodeled* feature at 3.54 keV. Also shown instrumental (upper) and astrophysical (lower) components of the background model. Right panel: Best fit value (black square) and $\Delta\chi^2 = 1, 4, 9$ contours for the line in the PN camera.

Camera	PN flux [10^{-6} cts/sec/cm 2]	Predicted flux [10^{-6} cts/sec/cm 2]	$\Delta\chi^2$
MOS1, PN best-fit	1.65	0.97	1.58
MOS2, PN best-fit	1.65	1.74	2.23
MOS1, PN 1σ lower	0.95	0.56	0.27
MOS2, PN 1σ lower	0.95	1.00	0.25

Table 2: Consistency check of MOS1 and MOS2 cameras with rescaled flux from PN camera. Line position is allowed to vary within 1σ bound for PN, i.e. 3.49–3.60 keV. See also Figures 3 and 4.

metals. In order to get as accurate a continuum model as possible, we have included these weak detector lines as narrow **gaussian** components in our spectral model.

The MOS1 camera reveals no other lines in the region 3–4 keV, see left panel in Figure 3. The MOS2 camera has a hint of a residual ($\Delta\chi^2 = 1.2$) in the position 3.60 ± 0.07 keV, see left Figure 4. Assuming that the line detected in the PN camera is a physical line, we rescale the PN flux, given by Eq. (1), according to the ratio of MOS1 and MOS2 FoV to that of the PN camera (see Table 1). Table 2 also shows change in the χ^2 when one adds a line with a fixed flux to the spectrum of MOS1 and MOS2 (allowing its position to vary within $\pm 1\sigma$ – from 3.49 to 3.60 keV). Clearly the observation of the line in the PN camera and non-observation in MOS1 and MOS2 are consistent at $\lesssim 1\sigma$ level.

3 Discussion

We analysed 26 observations of Draco dSph performed with the *XMM-Newton* during its AO14 programme. We find a 2.3σ significant positive line-like residual at $E = 3.54 \pm 0.06$ keV in the PN spectrum. A positive 1σ residual is also seen at the position $E = 3.60 \pm 0.07$ keV with the flux $F_{\text{MOS2}} = (0.76 \pm 0.66) \times 10^{-6}$ cts/sec/cm 2 . Their centroids are within 1σ as the right panel of Fig. 4 illustrates. The MOS1 camera had the lowest statistics due to the loss of two CCDs. It does not show the line but the absence of the signal is consistent with PN and MOS2 at 1σ level. Having shown that the three

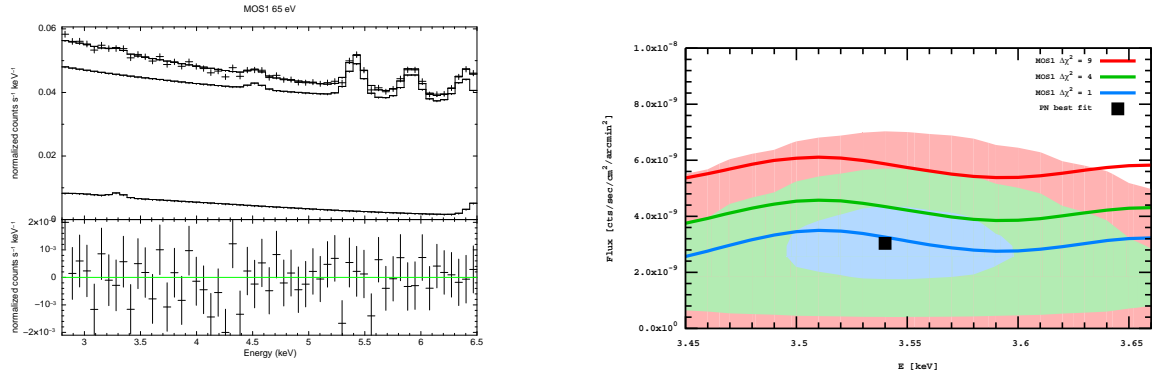


Figure 3: *Left panel:* MOS1 spectrum and residuals. *Right panel:* $\Delta\chi^2 = 1, 4, 9$ contours from the MOS1 camera (thick lines). The PN camera contours with $\Delta\chi^2 = 1, 4, 9$ are shown as shaded regions (identical to the contours in Fig. 2).

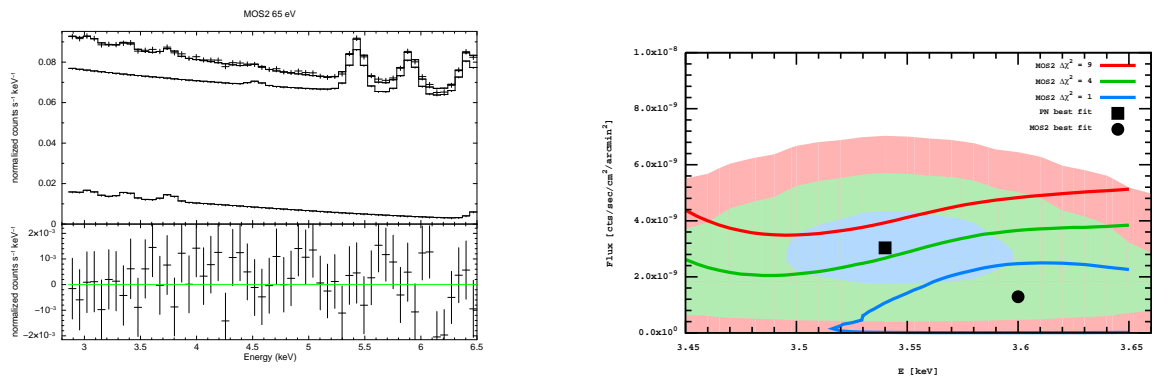


Figure 4: *Left panel:* MOS2 spectrum with *unmodeled* feature at ~ 3.5 keV and residuals. *Right panel:* $\Delta\chi^2 = 1, 4, 9$ contours from the MOS2 camera (thick lines) and the best fit value (black circle). The PN camera contours with $\Delta\chi^2 = 1, 4, 9$ are shown as shaded regions (identical to the contours in Fig. 2).

XMM cameras are consistent with each other, we now perform a common fit of all three. We kept the ratio of the `gaussian` normalisations at ~ 3.5 keV fixed to the ratios of the corresponding FoVs. The common fit finds a positive residual with $\Delta\chi^2 = 2.9$ at $E = 3.60 \pm 0.06$ keV and the flux $F = 1.3^{+0.9}_{-0.7} \times 10^{-9}$ cts/sec/cm²/arcmin². The resulting flux is compatible with the best-fit PN flux (Eq. (1)) at a 2σ level. As it is unclear how the common fit is affected by the uncertainties of cross-calibration between the three cameras, and because we are conservatively interested in this paper in exclusion rather than detection, we will use as our main result the 2σ upper bound from the common fit $F_{2\sigma} < 2.9 \times 10^{-9}$ cts/sec/cm²/arcmin², which approximately coincides with the best-fit PN flux, see Fig. 5.

If one interprets this signal as a line from the dark matter decay, its flux is related to the dark matter particle's lifetime τ_{DM} via

$$F = \frac{M_{\text{fov}}}{4\pi D_L^2} \frac{1}{\tau_{\text{DM}} m_{\text{DM}}} = \frac{\Omega_{\text{fov}}}{4\pi} \mathcal{S}_{\text{DM}} \frac{1}{\tau_{\text{DM}} m_{\text{DM}}} \quad (2)$$

where m_{DM} is the DM particle mass (equal to $2 \times E_{\text{line}}$), M_{fov} is the DM mass in the

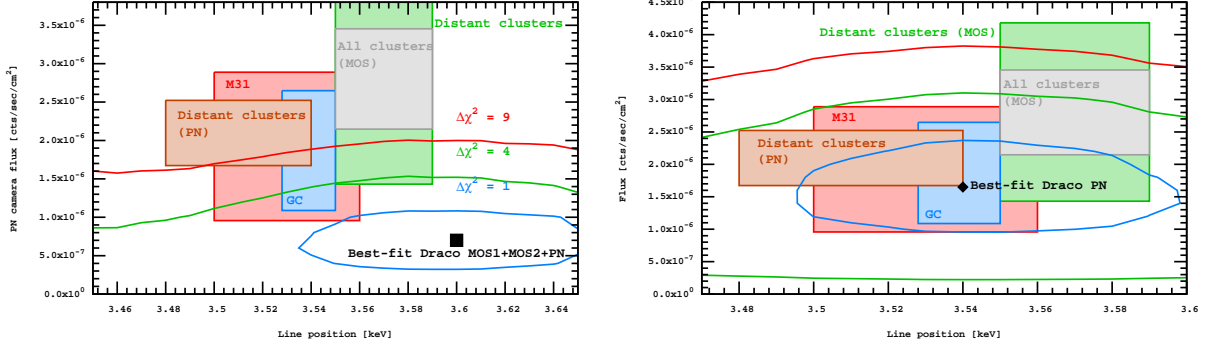


Figure 5: *Left*: Common fit to the MOS1, MOS2, and PN cameras (see text for details). The normalization of the 3.5 keV line between cameras is fixed according to the Ω_{fov} ratios (see Table 1). Filled rectangles show the range of fluxes predicted from previous works. The sizes of the regions take into account $\pm 1\sigma$ errors on the measured line fluxes and positions. The height of the rectangles also reflects additional spread in expected DM signals from the specified objects. The previous bounds are based on: [1] (“All clusters” and “Distant clusters” samples), [2] (“M31”) and [5] (“GC”). In particular, for “All clusters” and “Distant clusters” samples, we included an additional 20% uncertainty on its expected DM signal compared to the average values shown in Table 5 of [1]. *Right*: same as the left panel, but showing the Draco best fit for the PN camera only and the corresponding $\Delta\chi^2$ contours (note the different x and y ranges).

field-of-view of the camera, D_L is the luminosity distance, and in the second equality we introduced the *average DM column density*, \mathcal{S}_{DM} within the FoV Ω_{fov} .

The expected DM signal from Draco dSph is estimated based on the most recent stellar kinematics data, modeled in [21]. The average column density of Draco within the central $14'$ is $\mathcal{S}_{\text{Draco}} = 168 M_{\odot}/\text{pc}^2$ (with a typical error of $\sim 20\%$ [21]). An additional contribution from the Milky Way halo in the direction of the Draco dSph was adopted at the level of $\mathcal{S}_{\text{MW}} = 93 M_{\odot}/\text{pc}^2$ – based on the profile of [23]. The scatter in the values of the MW column density ranges from $56 M_{\odot}/\text{pc}^2$ [24] to $141 M_{\odot}/\text{pc}^2$ [25]. The resulting column density we adopt in the direction of Draco is $\mathcal{S}_{\text{Draco}} = 261^{+82}_{-65} M_{\odot}/\text{pc}^2$.

The corresponding lifetime, inferred from the Draco PN camera observation is

$$\tau_{\text{Draco}} = \begin{cases} 9.6^{+7.1}_{-2.8} \times 10^{27} \text{sec} & \text{for } \mathcal{S}_{\text{Draco}} = (168 + 93) M_{\odot}/\text{pc}^2 \\ 7.2^{+5.3}_{-2.1} \times 10^{27} \text{sec} & \text{for } \mathcal{S}_{\text{Draco}} = (140 + 56) M_{\odot}/\text{pc}^2 \\ 12.6^{+9.3}_{-3.7} \times 10^{27} \text{sec} & \text{for } \mathcal{S}_{\text{Draco}} = (202 + 141) M_{\odot}/\text{pc}^2 \end{cases} \quad (3)$$

Is this lifetime of this line compatible with the previous observations of 3.5 keV line? The answer is affirmative (see Fig. 5). The comparison of the region depends on both uncertainty of the flux measurement and the column density, \mathcal{S}_{M31} . The DM column density in the central $14'$ has been estimated in [2, 26, 27] and references therein. In this work, we adopt two values of \mathcal{S}_{M31} : $\mathcal{S}_{\text{M31,med}} = 600 M_{\odot}/\text{pc}^2$ (based on [28]) and $\mathcal{S}_{\text{M31,max}} = 1000 M_{\odot}/\text{pc}^2$ (based on [29, 30], see [26, 27] for the discussion of various profiles). The typical errors on M31 column densities are at the order of 50%. Notice, that a maximal disk large core profile of [31] having $\mathcal{S} \approx 120 M_{\odot}/\text{pc}^2$ would be incompatible with DM interpretation of the signal. The predicted lifetime would be too short to be consistent with the strength of the signal. This reiterates the conclusion, already made in [5] – the dark matter interpretation of the 3.5 keV line holds only if the density profiles of spiral galaxies (M31 and Milky Way) are cuspy.

Object/ Camera	Observed flux [10^{-6} cts/sec/cm 2]	\mathcal{S}_{DM} [M_{\odot}/pc^2]	τ_{DM} 10^{27} sec	Predicted flux [10^{-6} cts/sec/cm 2]		
				MOS1	MOS2	PN
M31 (MOS)	$4.9^{+1.6}_{-1.3}$	600	$7.3^{+2.6}_{-1.8}$	$1.28^{+0.42}_{-0.34}$	$2.31^{+0.76}_{-0.61}$	$2.20^{+0.72}_{-0.58}$
		1000	$12.2^{+4.4}_{-3.0}$	$0.77^{+0.25}_{-0.20}$	$1.38^{+0.45}_{-0.37}$	$1.32^{+0.43}_{-0.35}$
73 (all) stacked clusters (MOS) [1]	$4.0^{+0.8}_{-0.8}$	430	$5.7^{+1.7}_{-1.5}$	$1.65^{+0.59}_{-0.38}$	$2.98^{+1.06}_{-0.68}$	$2.82^{+1.01}_{-0.65}$
69 (distant) stacked clusters (MOS) [1]	$2.1^{+0.4}_{-0.5}$	255	$6.8^{+2.1}_{-2.1}$	$1.38^{+0.43}_{-0.43}$	$2.50^{+0.77}_{-0.77}$	$2.36^{+0.73}_{-0.73}$
Perseus with core (MOS) [1]	$52.0^{+24.1}_{-15.2}$	682	$0.75^{+0.23}_{-0.27}$	$12.5^{+7.0}_{-2.9}$	$22.7^{+12.8}_{-5.3}$	$21.4^{+12.0}_{-5.0}$
GC (MOS) [32]	24^{+12}_{-11}	3370 [33]	$7.9^{+6.7}_{-2.6}$	$1.19^{+0.58}_{-0.55}$	$2.15^{+1.05}_{-0.99}$	$2.03^{+1.00}_{-0.93}$

Table 3: Predicted line flux based on works [1, 2, 5]. The value for the Draco-deduced lifetime, τ_{Draco} is show in Eq. (3).

The DM distributions in Galactic Center region has been summarized in [5]. As a DM column density proxy, we used the distribution of [33] that gives $\mathcal{S}_{\text{GC}} = 3370 M_{\odot}/\text{pc}^2$. The spread of allowed values of column density for the Galactic Center distributions is larger than the order of magnitude, see Fig. 2 of [5].

Ref. [34] analysed Milky Way-like halo in Aquarius simulation, identified there DM halos that could be considered as hosting Draco dSph. It was found that the best agreement between the simulations and observational constraints is for $\tau \sim (6 - 10) \times 10^{27}$ sec (with which the Draco-deduced lifetime (3) is fully consistent). They also predicted the ratio of fluxes $F_{\text{Draco}}/F_{\text{GC}}$ to peak at 0.09 with the scatter ranging from 0.04 to 0.2 (95% range). Again, the ratio of the fluxes (~ 0.07) is close to the most probably value predicted by [34].

The dark matter column density of the combined sample of galaxy clusters is given by Table 5 of [1]. For the sample of “all distant clusters” considered here, the mean value of DM column density is $\mathcal{S}_{\text{clusters}} = 255 M_{\odot}/\text{pc}^2$ and we assign an additional 20% error to this data (notice that the relative errorbars on central column densities are at the order of ~ 2 , see e.g. Table I of [9]). The resulting lifetime is again listed in Table 3 and is consistent with our measurements.

Finally, a number of works [1, 5, 8, 35] already observed that the line from the central region of Perseus galaxy cluster is too strong to be compatible with other detections. This signal can only be reconciled with the simple decaying DM hypothesis either if there is a strong additional emission from the atomic lines (e.g., Ar XVII satellite line [1]) in the central region, or if there is a clump of dark matter, making the central column density much larger than estimated based on the temperature profiles [1]. The forthcoming Astro-H mission [15, 17, 36] will be able to resolve the issue with the origin of the emission from the Perseus center, both in core and outskirts, as well as in other bright clusters. On the other hand, outskirts of the Perseus cluster, considered in [2] are compatible with the decaying DM interpretation for lifetimes up to 8×10^{27} sec, compatible with Draco-deduced lifetime within 1σ .

In the recent paper [37] (JP15 in what follows), different results of the analysis of the same Draco dSph data have been reported. It is difficult to explain the discrepancies with our results without knowing the details of their data analysis. But we expect that the combination of the following factors may be important here. (i) The continuum

model of JP15 does not include the extragalactic `powerlaw` component, which affects the shape of the continuum in the 3–4 keV range at the level of a few % in a non-trivial, non-monotonic way due to the energy dependence of the effective area. *(ii)* The lines at ~ 3.3 keV and 3.7 keV are detected but unmodeled in JP15. Again, this increases the best-fit continuum level in the energy range 3–4 keV, which would artificially strengthen the upper bound on a 3.5 keV line. *(iii)* JP15 give the highest weight to their more stringent MOS upper limit. As we see in our spectra, the PN camera shows a positive $\sim 2\sigma$ residual at the expected line energy. When searching for weak signals at or below the telescope sensitivity, it is statistically proper to combine results from the independent detectors (provided they are mutually consistent), as we do. There is no reason to neglect the PN constraint – especially since in this case it is the most sensitive camera of the three, even with the shortest clean exposure.

Acknowledgements. We would like to thank K. Abazajian, G. Bertone, A. Geringer-Sameth, M. Lovell, M. Walker, C. Weniger for collaboration, discussion and useful comments. E. B. acknowledges support by NASA through grant NNX123AE77G. The work of D. I. has been partially supported from the Swiss National Science Foundation grant SCOPE IZ7370-152581, the grant No. F64/42-2015 of the State Fund for Fundamental Research of Ukraine, the Program of Cosmic Research of the National Academy of Sciences of Ukraine, and the State Programme of Implementation of Grid Technology in Ukraine. The Draco dSph observations were performed as a part of AO-14 Very Large Programme obtained with XMM-Newton, an ESA science mission with instruments and contributions directly funded by ESA Member States and NASA.

Appendix A. Data preparation and analysis

We analysed observations of Draco dSph performed in 2015 by the European Photon Imaging Cameras (EPIC) [22, 39] on-board of the X-ray Multi-Mirror Observatory *XMM-Newton* [40] as a part of AO-14 campaign (proposal 76480, PI: A. Boyarsky). The 1.4 Ms total requested exposure was divided into 26 observations (Table 4). We processed these observations from raw data using Extended Source Analysis Software (ESAS) [41] provided as part of the *XMM-Newton* Science Analysis System SAS v.14.0.0, with calibration files current as of December 1, 2015. Time intervals affected by soft proton flares were rejected using ESAS procedure `mos-filter` with standard spectral cuts. This rejection removed $\sim 30\%$ ($\sim 50\%$) of raw exposure for MOS(PN) cameras, see Table 1, comparable to other methods described in e.g. Sec. 8.4.1 of [42]. While the exposure reduction is significant, our tests showed that the sensitivity to the line does not increase if we use less-rigorous cleaning, because of the resulting increase of the continuum brightness. We excised the unrelated X-ray point sources using the ESAS procedure `cheese`, which masks the spatial regions of the $\geq 36''$ radius. For each observation, exposures and fields-of-view after removal of proton flares and point sources are listed in Table 4 and briefly summarized in Table 1. Spectra and response matrices from MOS and PN cameras produced by ESAS procedure `mos-spectra` were then combined using FTOOL `addspec` and binned with FTOOL `grppha` by 65 eV to have excellent statistics ($\sim 1 - 2\%$ rms variation per bin – comparable to the expected line excess above the continuum) while still resolving

ObsID	Observation date	Cleaned exposure [ksec]			Cleaned FoV [arcmin ²]		
		MOS1	MOS2	PN	MOS1	MOS2	PN
0764800101	2015-03-18	31.6	36.0	12.4	320.7	573.7	553.1
0764800201	2015-04-05	26.1	27.6	17.2	315.4	571.5	549.0
0764800301	2015-03-26	23.9	28.2	13.5	319.4	575.2	549.8
0764800401	2015-03-28	41.3	42.0	30.5	316.8	571.6	545.3
0764800501	2015-04-07	47.5	49.5	24.7	314.6	567.1	543.4
0764800601	2015-04-09	52.5	52.0	38.9	314.2	568.5	542.9
0764800701	2015-06-15	54.2	54.5	47.7	312.9	566.3	530.0
0764800801	2015-04-19	25.4	29.3	12.8	320.3	573.7	554.8
0764800901	2015-04-25	36.0	44.2	16.5	318.3	574.3	550.7
0770180101	2015-04-27	34.1	35.9	20.9	323.8	579.5	548.2
0770180201	2015-05-25	51.9	53.4	32.4	314.2	569.4	541.2
0770180301	2015-07-01	52.5	54.8	47.4	311.4	565.9	535.2
0770180401	2015-06-18	50.5	50.1	40.3	315.4	564.1	536.2
0770180501	2015-07-31	49.1	50.2	41.0	315.6	571.0	538.9
0770180601	2015-09-01	46.6	49.0	26.2	318.5	573.9	548.7
0770180701	2015-08-22	38.0	38.5	25.2	320.1	572.8	546.8
0770180801	2015-09-03	64.2	65.8	48.0	322.1	577.9	537.7
0770190101	2015-09-23	18.1	19.5	0.9	334.1	590.5	566.5
0770190201	2015-09-25	18.8	20.1	9.3	322.3	579.5	553.9
0770190301	2015-09-21	22.5	24.8	11.6	324.1	578.6	554.0
0770190401	2015-09-11	50.1	50.0	40.2	328.2	583.9	565.8
0770190501	2015-10-11	30.8	31.5	20.3	320.2	576.8	542.9
0770190601	2015-10-15	7.6	11.2	4.6	329.1	584.0	553.8
0770190701	2015-10-17	43.7	45.0	35.5	320.5	572.8	537.4
0770190801	2015-10-19	31.7	32.5	22.4	326.2	583.2	547.2
0770180901	2015-10-13	19.2	20.8	11.4	324.6	579.1	560.9

Table 4: Cleaned exposures and fields-of-view for 26 AO14 observations of Draco dSph used in our analysis, see Appendix A. for details. The total clean exposure per camera as well as exposure weighted FoV is summarized in Table 1. Notable difference between MOS1 and MOS2 fields of view is due to micrometeoroid damages in MOS1, see e.g. [38].

the spectral lines. For PN camera, we additionally corrected the obtained spectra for out-of-time events using the standard procedure.

We stress that for our current purpose, given the low expected flux of the spectral line in question and the limited spectral resolution of the CCD detectors, accurate modeling of the continuum emission in the immediate vicinity of the line is crucial. For this, we must account for all the faint detector lines and features that may bias the continuum even at a percent level. We do this by creating a spectral model that includes the detector and sky X-ray background components as described below. We analyse the spectra in the band 2.8–10 keV (for MOS spectra) and 2.8–6.8 + 10–11 keV for PN spectra (to stay well away from the mirror edges found at $E \lesssim 2.5$ keV) using standard X-ray spectral fitting tool `Xspec`. The region 6.8–10 keV was removed from PN camera to avoid modeling very strong instrumental lines (Ni $K\alpha$, Cu $K\alpha$, Ni $K\beta$ and Zn $K\alpha$), see Table 5 that that cannot be modeled adequately with simple Gaussian profiles at such good statistics. However, adding the high energy bins (at 10–11 keV) allows us to constrain the slope of the instrumental continuum.

The instrumental background is modeled by a sum of unfolded broken `powerlaw` continuum and several narrow `gaussians` corresponding to bright fluorescent lines originated inside the instrument. Because astrophysical emission from dwarf spheroidal galaxies is negligible [27, 43–47], astrophysical model represents contribution of Cosmic X-ray background (CXB) modeled by a folded `powerlaw` continuum. The flux and powerlaw index of Cosmic X-ray background were tied consistent to previous studies summarized in e.g. [48]. Neutral hydrogen absorption column density was fixed to the weighted value $n_{\text{H}} = 2.25 \times 10^{20} \text{ cm}^{-2}$ obtained from Leiden-Argentine-Bonn survey [49] in direction of Draco.

References

- [1] E. Bulbul, M. Markevitch, A. Foster, R. K. Smith, M. Loewenstein and S. W. Randall, *Detection of an Unidentified Emission Line in the Stacked X-Ray Spectrum of Galaxy Clusters*, *ApJ* **789** (July, 2014) 13 [1402.2301].
- [2] A. Boyarsky, O. Ruchayskiy, D. Iakubovskiy and J. Franse, *Unidentified Line in X-Ray Spectra of the Andromeda Galaxy and Perseus Galaxy Cluster*, *Physical Review Letters* **113** (Dec., 2014) 251301 [1402.4119].
- [3] D. A. Iakubovskiy, *New emission line at ~ 3.5 keV - observational status, connection with radiatively decaying dark matter and directions for future studies*, *Advances in Astronomy and Space Physics* **4** (Dec., 2014) 9–14 [1410.2852].
- [4] S. Riemer-Sorensen, *Questioning a 3.5 keV dark matter emission line*, *ArXiv e-prints* (May, 2014) [1405.7943].
- [5] A. Boyarsky, J. Franse, D. Iakubovskiy and O. Ruchayskiy, *Checking the Dark Matter Origin of a 3.53 keV Line with the Milky Way Center*, *Physical Review Letters* **115** (Oct., 2015) 161301 [1408.2503].

Parameter	MOS1	MOS2	PN
CXB powerlaw index	1.40 ^{+0.32} _{-0.06}	1.36 ^{+0.07} _{-0.08}	1.61 ^{+0.13} _{-0.06}
CXB powerlaw flux at 2-10 keV [10^{-11} erg/sec/cm ² /deg ²]	1.37 ^{+0.34} _{-0.67}	1.40 ^{+0.30} _{-0.40}	2.03 ^{+0.38} _{-0.30}
Instrumental background powerlaw index	0.31	0.26	0.36
Extra gaussian line position at ~ 3.0 keV [keV]	—	3.045	—
K K α line ^a position [keV]	3.295	3.380	—
Ca K α line ^a position [keV]	—	3.770	—
Ti K α line position [keV]	4.530	—	4.530
Cr K α line position [keV]	5.420	5.431	5.445
Mn K α line position [keV]	5.919	5.901	5.910
Fe K α line position [keV]	6.386	6.424	6.395
Fe K β line position [keV]	7.128	7.148	n/i ^a
Ni K α line position [keV]	7.460	7.479	n/i ^a
Cu K α line position [keV]	8.021	8.045	n/i ^a
Ni K β line position [keV]	8.251	8.267	n/i ^a
Zn K α line position [keV]	8.620	8.629	n/i ^a
Au L α line position [keV]	9.716	9.710	n/i ^a
Overall quality of fit (χ^2 /dof)	73.8/86	79.3/75	47.0/58

Table 5: Model parameters for MOS1, MOS2 and PN cameras.

^a In PN, bright instrumental lines at 7-10 keV are not included (n/i) to our model due to large residuals appearing when these lines are modeled. Instead, we included high-energy range above 10 keV to our PN to improve the instrumental continuum modeling.

- [6] T. Jeltema and S. Profumo, *Discovery of a 3.5 keV line in the Galactic Centre and a critical look at the origin of the line across astronomical targets*, MNRAS **450** (June, 2015) 2143–2152 [1408.1699].
- [7] E. Carlson, T. Jeltema and S. Profumo, *Where do the 3.5 keV photons come from? A morphological study of the Galactic Center and of Perseus*, JCAP **2** (Feb., 2015) 9 [1411.1758].
- [8] O. Urban, N. Werner, S. W. Allen, A. Simionescu, J. S. Kaastra and L. E. Strigari, *A Suzaku search for dark matter emission lines in the X-ray brightest galaxy clusters*, MNRAS **451** (Aug., 2015) 2447–2461 [1411.0050].
- [9] D. Iakubovskiy, E. Bulbul, A. R. Foster, D. Savchenko and V. Sadova, *Testing the origin of ~ 3.55 keV line in individual galaxy clusters observed with XMM-Newton*, ArXiv e-prints (Aug., 2015) [1508.05186].
- [10] D. Malyshev, A. Neronov and D. Eckert, *Constraints on 3.55 keV line emission from stacked observations of dwarf spheroidal galaxies*, Phys.Rev. **D90** (Aug., 2014) 103506 [1408.3531].
- [11] M. E. Anderson, E. Churazov and J. N. Bregman, *Non-detection of X-ray emission from sterile neutrinos in stacked galaxy spectra*, MNRAS **452** (Oct., 2015) 3905–3923 [1408.4115].

- [12] E. Figueroa-Feliciano, A. J. Anderson, D. Castro, D. C. Goldfinger, J. Rutherford, M. E. Eckart, R. L. Kelley, C. A. Kilbourne, D. McCammon, K. Morgan, F. S. Porter, A. E. Szymkowiak and XQC Collaboration, *Searching for keV Sterile Neutrino Dark Matter with X-Ray Microcalorimeter Sounding Rockets*, ApJ **814** (Nov., 2015) 82 [1506.05519].
- [13] N. Sekiya, N. Y. Yamasaki and K. Mitsuda, *A search for a keV signature of radiatively decaying dark matter with Suzaku XIS observations of the X-ray diffuse background*, PASJ (Sept., 2015) [1504.02826].
- [14] L. Gu, J. Kaastra, A. J. J. Raassen, P. D. Mullen, R. S. Cumbee, D. Lyons and P. C. Stancil, *A novel scenario for the possible X-ray line feature at ~ 3.5 keV. Charge exchange with bare sulfur ions*, A&A **584** (Dec., 2015) L11 [1511.06557].
- [15] K. Mitsuda, R. L. Kelley, H. Akamatsu, T. Bialas, K. R. Boyce, G. V. Brown, E. Canavan, M. Chiao, E. Costantini, J.-W. den Herder and et al., *Soft x-ray spectrometer (SXS): the high-resolution cryogenic spectrometer onboard ASTRO-H*, in *Society of Photo-Optical Instrumentation Engineers (SPIE) Conference Series*, vol. 9144 of *Society of Photo-Optical Instrumentation Engineers (SPIE) Conference Series*, p. 2, July, 2014.
- [16] K. Koyama, J. Kataoka, M. Nobukawa, H. Uchiyama, S. Nakashima, F. Aharonian, M. Chernyakova, Y. Ichinohe, K. K. Nobukawa, Y. Maeda and et al. for the ASTRO-H Science Working Group, *ASTRO-H White Paper - Plasma Diagnostic and Dynamics of the Galactic Center Region*, ArXiv e-prints (Dec., 2014) [1412.1170].
- [17] T. Kitayama, M. Bautz, M. Markevitch, K. Matsushita, S. Allen, M. Kawaharada, B. McNamara, N. Ota, H. Akamatsu, J. de Plaa and et al. on behalf of the ASTRO-H Science Working Group, *ASTRO-H White Paper - Clusters of Galaxies and Related Science*, ArXiv e-prints (Dec., 2014) [1412.1176].
- [18] D. Iakubovskiy, *Checking the potassium origin of the new emission line at 3.5 keV using the K XIX line complex at 3.7 keV*, MNRAS **453** (Nov., 2015) 4097–4101 [1507.02857].
- [19] A. Boyarsky, A. Neronov, O. Ruchayskiy and I. Tkachev, *Universal Properties of Dark Matter Halos*, Physical Review Letters **104** (May, 2010) 191301 [0911.3396].
- [20] A. Boyarsky, O. Ruchayskiy, D. Iakubovskiy, A. V. Maccio' and D. Malyshev, *New evidence for dark matter*, ArXiv e-prints (Nov., 2009) [0911.1774].
- [21] A. Geringer-Sameth, S. M. Koushiappas and M. Walker, *Dwarf Galaxy Annihilation and Decay Emission Profiles for Dark Matter Experiments*, ApJ **801** (Mar., 2015) 74 [1408.0002].
- [22] L. Strüder, U. Briel, K. Dennerl, R. Hartmann, E. Kendziorra, N. Meidinger, E. Pfeffermann, C. Reppin, B. Aschenbach, W. Bornemann and et al., *The European Photon Imaging Camera on XMM-Newton: The pn-CCD camera*, A&A **365** (Jan., 2001) L18–L26.

- [23] M. Weber and W. de Boer, *Determination of the local dark matter density in our Galaxy*, *A&A* **509** (Jan., 2010) A25 [0910.4272].
- [24] X. Xue *et. al.*, *The Milky Way's Circular Velocity Curve to 60 kpc and an Estimate of the Dark Matter Halo Mass from Kinematics of 2400 SDSS Blue Horizontal Branch Stars*, *Astrophys.J.* **684** (Sept., 2008) 1143–1158 [0801.1232].
- [25] F. Nesti and P. Salucci, *The Dark Matter halo of the Milky Way, AD 2013*, *JCAP* **1307** (July, 2013) 016 [1304.5127].
- [26] A. Boyarsky, D. Iakubovskiy, O. Ruchayskiy and V. Savchenko, *Constraints on decaying Dark Matter from XMM-Newton observations of M31*, *Mon.Not.Roy.Astron.Soc.* **387** (2008) 1361 [0709.2301].
- [27] A. Boyarsky, O. Ruchayskiy, D. Iakubovskiy, M. G. Walker, S. Riemer-Sørensen and S. H. Hansen, *Searching for dark matter in X-rays: how to check the dark matter origin of a spectral feature*, *MNRAS* **407** (Sept., 2010) 1188–1202 [1001.0644].
- [28] L. M. Widrow and J. Dubinski, *Equilibrium disk-bulge-halo models for the Milky Way and Andromeda galaxies*, *Astrophys.J.* **631** (Oct., 2005) 838–855 [astro-ph/0506177].
- [29] J. Geehan, M. A. Fardal, A. Babul and P. Guhathakurta, *Investigating the Andromeda Stream. 1. Simple analytic bulge-disk-halo model for M31*, *Mon.Not.Roy.Astron.Soc.* **366** (Mar., 2006) 996–1011 [astro-ph/0501240].
- [30] E. Tempel, A. Tamm and P. Tenjes, *Visible and dark matter in M31. 2. A dynamical model and dark matter density distribution*, *Mon.Not.Roy.Astron.Soc.* **707** (July, 2007) [0707.4374].
- [31] E. Corbelli, S. Lorenzoni, R. A. Walterbos, R. Braun and D. A. Thilker, *A wide-field HI mosaic of Messier 31. II. The disk warp, rotation and the dark matter halo*, *Astron.Astrophys.* **511** (Feb., 2010) A89 [0912.4133].
- [32] A. Boyarsky, J. Franse, D. Iakubovskiy and O. Ruchayskiy, *Comment on the paper "Dark matter searches going bananas: the contribution of Potassium (and Chlorine) to the 3.5 keV line" by T. Jeltema and S. Profumo*, *ArXiv e-prints* (Aug., 2014) [1408.4388].
- [33] M. C. Smith, G. R. Ruchti, A. Helmi, R. F. G. Wyse, J. P. Fulbright, K. C. Freeman, J. F. Navarro, G. M. Seabroke, M. Steinmetz, M. Williams and *et al.*, *The RAVE survey: constraining the local Galactic escape speed*, *MNRAS* **379** (Aug., 2007) 755–772 [astro-ph/0611671].
- [34] M. R. Lovell, G. Bertone, A. Boyarsky, A. Jenkins and O. Ruchayskiy, *Decaying dark matter: the case for a deep X-ray observation of Draco*, *ArXiv e-prints* (Nov., 2014) [1411.0311].

- [35] T. Tamura, R. Iizuka, Y. Maeda, K. Mitsuda and N. Y. Yamasaki, *An X-ray spectroscopic search for dark matter in the Perseus cluster with Suzaku*, PASJ **67** (Apr., 2015) 23 [1412.1869].
- [36] T. Takahashi, K. Mitsuda, R. Kelley, H. Aarts, F. Aharonian, H. Akamatsu, F. Akimoto, S. Allen, N. Anabuki, L. Angelini and et al., *The ASTRO-H X-ray Observatory*, in *Society of Photo-Optical Instrumentation Engineers (SPIE) Conference Series*, vol. 8443 of *Society of Photo-Optical Instrumentation Engineers (SPIE) Conference Series*, p. 1, Sept., 2012. 1210.4378.
- [37] T. E. Jeltema and S. Profumo, *Deep XMM Observations of Draco rule out a dark matter decay origin for the 3.5 keV line*, *ArXiv e-prints* (Dec., 2015) [1512.01239].
- [38] T. Abbey, J. Carpenter, A. Read, A. Wells, Xmm Science Centre and Swift Mission Operations Center, *Micrometeoroid Damage to CCDs in XMM-Newton and Swift and its Significance for Future X-ray Missions*, in *The X-ray Universe 2005* (A. Wilson, ed.), vol. 604 of *ESA Special Publication*, p. 943, Jan., 2006.
- [39] M. J. L. Turner, A. Abbey, M. Arnaud, M. Balasini, M. Barbera, E. Belsole, P. J. Bennie, J. P. Bernard, G. F. Bignami, M. Boer and et al., *The European Photon Imaging Camera on XMM-Newton: The MOS cameras : The MOS cameras*, A&A **365** (Jan., 2001) L27–L35 [astro-ph/0011498].
- [40] F. Jansen, D. Lumb, B. Altieri, J. Clavel, M. Ehle, C. Erd, C. Gabriel, M. Guainazzi, P. Gondoin, R. Much and et al., *XMM-Newton observatory. I. The spacecraft and operations*, A&A **365** (Jan., 2001) L1–L6.
- [41] K. D. Kuntz and S. L. Snowden, *The EPIC-MOS particle-induced background spectra*, A&A **478** (Feb., 2008) 575–596.
- [42] D. Iakubovskiy, *Constraining properties of dark matter particles using astrophysical data*. PhD thesis, Instituut-Lorentz for Theoretical Physics, 2013.
- [43] J. E. Gizis, J. R. Mould and S. Djorgovski, *An X-ray image of the Fornax dwarf spheroidal galaxy*, PASP **105** (Aug., 1993) 871–874.
- [44] A. Boyarsky, J. Nevalainen and O. Ruchayskiy, *Constraints on the parameters of radiatively decaying dark matter from the dark matter halos of the Milky Way and Ursa Minor*, A&A **471** (Aug., 2007) 51–57 [arXiv:astro-ph/0610961].
- [45] T. E. Jeltema and S. Profumo, *Searching for Dark Matter with X-Ray Observations of Local Dwarf Galaxies*, ApJ **686** (Oct., 2008) 1045–1055 [0805.1054].
- [46] S. Riemer-Sørensen and S. H. Hansen, *Decaying dark matter in the Draco dwarf galaxy*, A&A **500** (June, 2009) L37–L40.
- [47] E. Sonbas, B. Rangelov, O. Kargaltsev, K. S. Dhuga, J. Hare and I. Volkov, *X-ray Sources in the Dwarf Spheroidal Galaxy Draco*, *ArXiv e-prints* (May, 2015) [1505.00216].

- [48] A. Moretti, C. Pagani, G. Cusumano, S. Campana, M. Perri, A. Abbey, M. Ajello, A. P. Beardmore, D. Burrows, G. Chincarini, O. Godet, C. Guidorzi, J. E. Hill, J. Kennea, J. Nousek, J. P. Osborne and G. Tagliaferri, *A new measurement of the cosmic X-ray background*, *A&A* **493** (Jan., 2009) 501–509.
- [49] P. M. W. Kalberla, W. B. Burton, D. Hartmann, E. M. Arnal, E. Bajaja, R. Morras and W. G. L. Pöppel, *The Leiden/Argentine/Bonn (LAB) Survey of Galactic HI. Final data release of the combined LDS and IAR surveys with improved stray-radiation corrections*, *A&A* **440** (Sept., 2005) 775–782 [[astro-ph/0504140](#)].